

The surface boundary layer of a hurricane. II

By L. M. LESLIE and R. K. SMITH, *Department of Mathematics, Monash University, Clayton, Victoria 3168, Australia*

(Manuscript received June 6, 1969; revised version February 13, 1970)

ABSTRACT

In an earlier paper, a momentum integral method was developed by one of the authors (Smith, 1968) to investigate the gross features of the surface friction layer of a steady, axisymmetric hurricane, which is specified by its radial pressure variation near the sea surface. Thus, by choosing suitable vertical profiles of inflow and swirling velocity components in the boundary layer, the technique provides estimates for the radial distribution of mean inflow, of boundary layer thickness and of mean upflow through the top of the layer. It therefore gives a measure of the constraint imposed by the inflow layer on the vortex which produces it.

In the present work, the method is used to investigate the effects of turbulent structure on the boundary layer characteristics. The turbulence is represented by an eddy viscosity K_M , and solutions corresponding to a variety of models for the variation of K_M , together with an appropriate surface boundary condition, are compared. These models range from an eddy viscosity which is everywhere constant and with the condition of no-slip at the surface, to a K_M which has both radial and vertical structure and which varies linearly with height in the first few tens of metres above the sea surface. In the latter case, one is able to parameterize the roughness of the sea surface.

The solutions indicate that in actual hurricanes, an increase of K_M towards the region of maximum winds produces a significant increase in the upflow compared with a similar layer in which K_M has no radial variation. Moreover, the radial profile of boundary layer thickness differs markedly between the two cases. Solutions for three surface boundary conditions are compared and the volume inflow and upflow rates at a given radius are also found to increase with an increase in the constraint at the sea surface, that is, with an increase in surface stress.

An error in one of the calculations of the first paper is also resolved.

Introduction

The importance of the surface boundary layer on the dynamics of a hurricane is due to the constraint it imposes on the meridional circulation of the vortex, by producing a strong coupling between the azimuthal and vertical velocity fields. The reasons for this constraint are discussed by Smith (1968), henceforth denoted by I. In this, the author develops a momentum integral method which can be used to study the development of the boundary layer from the outer reaches of the vortex to the central regions of high swirling wind speeds. The flow above the boundary layer is represented by a steady, inviscid, circular vortex, with zero radial flow and azimuthal velocity $V_{gr}(R)$, specified by the gradient wind equation with a suitably chosen radial pressure profile $P(R)$, where R measures radial distance from the axis of

symmetry. In the absence of horizontal boundaries, a vortex of this kind can support an arbitrary radial distribution of axial flow with velocity $W_{gr}(R)$. However, in the presence of such a boundary and with V_{gr} given, the upflow W_{gr} is determined uniquely by the boundary layer flow. The momentum integral method is an approximate one in which the boundary layer equations are integrated across the layer with respect to height Z , say. Vertical velocity profiles are specified and these must satisfy the appropriate conditions at the boundary itself and at the upper edge of the layer. The integrated equations are then used to calculate the radial variation of inflow velocity and boundary layer thickness. The upflow velocity is obtained from an integrated form of the continuity equation. The final equations consist of a pair of first-order ordinary differential equations for a

scale boundary layer thickness $\delta(R)$ and the amplitude coefficient $E(R)$, of a scale inflow velocity $E(R) V_{gr}(R)$. The two equations are readily solved if the dependent variables δ and E are known at a given radius, R_g say. In I, R_g is taken to be sufficiently far from the storm centre (in fact, 1000 km) so that the wind speed above the boundary layer $V_g (= V_{gr}(R_g))$ is light and the flow there is approximately geostrophic. At this radius, the boundary layer approximates to an Ekman-type layer, the solution for which is known. This solution is used to define $\delta(R_g)$ and $R(R_g)$ and similar velocity profiles are taken in the momentum integral equations, but with scales $\delta(R)$ and $E(R)$. The equations are then integrated numerically from R_g to smaller radii.

In I, two surface boundary conditions are examined; these are,

- (A) when there is no slip at the sea surface and the sea is assumed to be at rest, and
- (B) when the surface stress is in the direction of the surface wind. In addition, two forms are taken for K_M , namely
 - (i) when K_M is everywhere constant and
 - (ii) when K_M increases from 25 m²/sec by a factor of two between the geostrophic radius R_g , and the radius of maximum azimuthal wind R_m , but is constant with height.

Solutions are obtained in four cases corresponding to condition A or B with turbulent structure (i) or (ii).

The solution for the case B(i) showed an 'eruption' of the boundary layer at a considerable distance from the radius of maximum winds, with very weak inflow and upflow at smaller radii. This feature is not observed in hurricanes and it appeared that the profiles which are obtained in this case are especially sensitive to the values chosen for the parameters C_D , the drag coefficient, and K_M , since in the case B(ii) with K_M decreasing with radius, no 'eruption' occurred. This anomalous result prompted a more detailed investigation to test the sensitivity of the method to the particular choice of profile. During the early stages an erroneous sign was detected in one of the profiles for surface condition B¹ and with this corrected, the boundary layer solutions for cases B(i) and B(ii) resemble closely those for the

corresponding cases A, but the inflow is weaker in the first two solutions. This fact removes in some measure the basis for the rather pessimistic conclusions of I and it has been found possible to use the model developed in that paper to study a variety of representations for the turbulent structure and the surface boundary condition, in relation to the constraint they imply on the meridional circulation of a hurricane. The results of these investigations are discussed here.

The basic equations

We assume that K_M has both radial and vertical structure and write $K_M^* k(r, z)$, where K_M^* is a scale for K_M at the geostrophic radius R_g . The non-dimensional boundary layer equations may then be written in the form,

$$R_0 \left[\frac{d}{dr} \left(r \int_0^\infty u^2 dz \right) + \int_0^\infty (v_{gr}^2 - v^2) dz \right] + \int_0^\infty r(v_{gr} - v) dz = -r \left(k \frac{\partial u}{\partial z} \right)_{z=0}, \quad (1)$$

$$R_0 \left[\frac{d}{dr} \left(r^3 \int_0^\infty uv dz \right) + r^3 v_{gr} w_{gr} \right] + \int_0^\infty r^3 u dz = -r^3 \left(k \frac{\partial v}{\partial z} \right)_{z=0}, \quad (2)$$

where $R_0 = V_g/(R_g f)$ is a Rossby number appropriate to the flow at the geostrophic radius, f is the coriolis parameter, (u, v, w) are the velocity components in a cylindrical coordinate system (r, θ, z) and

$$w_{gr} = -\frac{1}{r} \frac{d}{dr} \left(r \int_0^\infty u dz \right), \quad (3)$$

is the vertical velocity at the upper edge of the boundary layer. Equations (1), (2) and (3) correspond to Eqs. (16), (17) and (18) in I. The dimensional length and velocity scales associated with r, z, u, v, w and v_{gr} $R_g, Z_g, V_g, V_g, Z_g V_g/R_g$ and V_g respectively, where $Z_g = (K_M/f)^{1/2}$

¹ The first line in Eq. (27), which was incorrectly numbered Eq. (23), should read

$$f(\eta) = -ce^{-\eta}(a_1 \sin \eta - a_2 \cos \eta).$$

is a vertical scale appropriate to the boundary layer flow at large radii, $R \geq 0(R_g)$.

Guided by the known Ekman solution in the limiting case $R_0 \rightarrow 0$ we take

$$\left. \begin{aligned} u(r, z) &= v_{gr}(r) E(r) f(\eta) \\ v(r, z) &= v_{gr}(r) g(\eta) \end{aligned} \right\}, \quad (4)$$

where $\eta = z/\delta(r)$, $\delta(r)$ is a non-dimensional scale boundary layer thickness, $E(r)$ is the amplitude coefficient of the radial velocity and $f(\eta)$, $g(\eta)$ are the velocity profiles across the flow.

If Eqs. (4) are substituted into Eqs. (1), (2) and (3), one obtains three equations for the radial variation of E , δ and w_{gr} . The calculations are simplified if E^2 and $E\delta^2$ are taken as dependent variables, in which case the equations read,

$$\frac{1}{E^2} \frac{d}{dr} (E^2) = -\frac{2}{r\tilde{v}^2} \left[\frac{d}{dr} (r\tilde{v}^2) - B\tilde{v} \frac{d}{dr} (r\tilde{v}) \right] - \left(\frac{2A}{r} + \frac{2X}{\tilde{v}} \right) \frac{1}{E^2} + \frac{2Y}{\tilde{v}} - \frac{2(C+D)}{\tilde{v}E\delta^2}, \quad (5)$$

$$\frac{1}{E\delta^2} \frac{d}{dr} (E\delta^2) = \frac{1}{r\tilde{v}} \left[\frac{d}{dr} (r\tilde{v}^2) - 3B\tilde{v} \frac{d}{dr} (r\tilde{v}) \right] + \left(\frac{A}{r} + \frac{X}{\tilde{v}} \right) \frac{1}{E^2} - \frac{3Y}{\tilde{v}} + \frac{C+D}{\tilde{v}E\delta^2}, \quad (6)$$

and

$$w_{gr} = -\frac{I_5}{R_0\delta} \left[D + E\delta^2 \left\{ \frac{(1-B)}{r} \frac{d}{dr} (r\tilde{v}) - Y \right\} \right], \quad (7)$$

where $\tilde{v} = R_0 v_{gr}$ and¹

$$A = \frac{I_2}{I_1}, \quad B = \frac{I_5 - 2I_4}{I_5 - I_4}, \quad C = \lim_{\eta \rightarrow 0} \frac{k(r, \sqrt{2}\eta) f'(\eta)}{I_1},$$

$$D = \lim_{\eta \rightarrow 0} \frac{k(r, \sqrt{2}\eta) g'(\eta)}{I_5 - I_4}, \quad X = \frac{I_3}{I_1}, \quad Y = \frac{I_5}{I_4 - I_5},$$

where

$$\left. \begin{aligned} I_1 &= \int_0^\infty f^2 d\eta, & I_2 &= \int_0^\infty (1-g^2) d\eta, \\ I_3 &= \int_0^\infty (1-g) d\eta, \\ I_4 &= \int_0^\infty fg d\eta, & I_5 &= \int_0^\infty f d\eta. \end{aligned} \right\} \quad (8)$$

¹ N.B. The expressions for C and D assume that for $k(1, z)$ variable, $k(r, z)\alpha z$ and hence $\alpha\eta$ as $z \rightarrow 0$. Moreover, C and D are functions of r if k is.

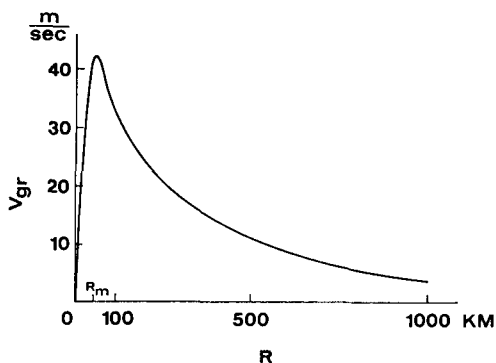


Fig. 1. The profile of swirl velocity V_{gr} , a at the top of the boundary layer.

The pressure and azimuthal velocity profiles which are taken to represent the vortex are the same as those used in I. Thus,

$$v = -\frac{1}{2}r + \left(\frac{1}{4}r^2 + \frac{mxb}{r} \exp xb(1-r^{-1}) \right)^{\frac{1}{2}},$$

where $m = \left(\frac{P_g - P_c}{\rho} \right) / (R_g^2 f^2),$

P_c and P_g are the pressure at the centre of the hurricane and at the geostrophic radius respectively, ρ is the density of air (assumed constant), $b = R_M/R_g$ and x satisfies the equation

$$mx(x-1)^2 e^{x(b-1)} - (2-x)b^2 = 0.$$

The calculations are performed following the same method as those in I and with the same hurricane vortex, i.e. $P_c = 940$ mb, $P_g = 1000$ mb, $R_g = 1000$ km, $R_M = 40$ km, $\rho = 0.0012$ g/c.c. and $f = 5 \times 10^{-5}$ sec⁻¹. In this case, the maximum azimuthal velocity is 43 m/sec and this decreases to about 4 m/sec at 1000 km to give a value of 7.8×10^{-2} for R_0 . The profile $V_{gr}(R)$ obtained from these values is shown in Fig. 1.

The velocity profiles

Far from the axis of the vortex the boundary layer flow is almost quasi-geostrophic ($R_0 < 1$) and the velocity profiles at $r = 1$ satisfy approximately the equations

$$1 - v = \frac{\partial}{\partial z} \left(k \frac{\partial u}{\partial z} \right), \quad (9)$$

$$u = \frac{\partial}{\partial z} \left(k \frac{\partial v}{\partial z} \right), \quad (10)$$

subject to the boundary condition

$$(u, v) \rightarrow (0, 1) \text{ as } z \rightarrow \infty \quad (11)$$

and an appropriate condition at $z = 0$, which in general will depend on the form chosen for $k(1, z)$. If radial variations of k can be ignored at large radii, $r \geq 0(1)$ —and it will be seen later that this is very reasonable—a solution to Eqs. (9) and (10) can be found which is independent of r . The profiles obtained for a given function $k(1, z)$ and with a corresponding surface condition are used to define profiles for $f(\eta)$ and $g(\eta)$. As in I, it is convenient to take

$$\left. \begin{aligned} f(\eta) &= u(1, \eta\sqrt{2}) \\ g(\eta) &= v(1, \eta\sqrt{2}) \end{aligned} \right\} \quad (12)$$

The cross-isobaric volume flux, given by the profile of u , is proportional to the azimuthal component of surface stress, $\tau_{0\theta}/\rho = (k\partial v/\partial z)_{z=0}$. This follows by integrating Eq. (10) with respect to z from $z = 0$ to $z = \infty$ provided that $(k\partial v/\partial z) \rightarrow 0$ as $z \rightarrow \infty$ and this condition is satisfied by the variations of k considered here.

The air sea boundary condition and turbulent structure

The purpose of this paper is to establish a basis for answering the questions: “how can one represent the turbulent structure and what is an appropriate surface boundary condition to describe the hurricane inflow layer?” Little guidance may be expected from observation at the extreme wind speeds and in the mountainous seas which occur around the central core of a hurricane. The best one can do is to follow the observational data obtained at more moderate wind speeds and hope that the representation of turbulent structure and surface condition based on these will not be grossly in error by extrapolation to stronger winds. In this paper we examine three possible representations. These are described below. They are all based on the observational data available¹ and involve varying degrees of approximation to reality, in each case consistent with the approximations made in selecting the model for the hurricane vortex itself.

Case A. The simplest representation takes K_M to be everywhere constant, equal to K_M^* say, and assumes no slip at the sea surface and the sea to be at rest. In this case the functions $f(\eta)$ and $g(\eta)$ are the classical Ekman profiles, given in complex form by $g + if = 1 - e^{-(1+i)\eta}$, and $\tau_{0\theta}/\rho = 1/\sqrt{2}$. Therefore, at large radii where local Rossby numbers $V_{gr}(R)/(Rf)$ are small, the boundary layer flow is almost geostrophic and the total inflow rate is approximately

$$(\frac{1}{2} K_M^* f)^\dagger V_{gr}.$$

An objection to this representation is as follows. The product of K_M with the local mean velocity gradient is, by definition, the stress τ/ρ across a horizontal surface due to the vertical exchange of horizontal momentum across this surface by turbulent fluctuations. In conditions of neutral stability and for moderate wind speeds (i.e. less than about 15 m/sec), it is well established observationally that $K_M = \kappa u_* Z$ in a sublayer which extends over the lowest few tens of metres of the atmosphere. In this formula, κ is Von-Kármán's constant which is found to have a value of approximately 0.4 and u_* is the friction velocity, defined in terms of the surface stress τ_0/ρ by $u_*^2 = |\tau_0/\rho|$. At larger heights, the variation of K_M with Z is open to dispute and about the most that can be said is that the variation is much slower than in the sublayer. Thus, to a first approximation we shall take K_M^* to be constant above the sublayer. By taking K_M to be constant through the sublayer as well and equal to its value at larger heights, we may considerably overestimate the stress at the surface and hence the inflow. Thus, in case A, by taking the Ekman profiles in the integrated equations (5) and (6), we might expect to calculate too much inflow throughout the entire inflow layer (unless, in actual hurricanes K_M has radial structure—see below). This situation could be averted by regarding K_M as a parameter for the inflow at large radii and choosing K_M^* to give a realistic value for this. However, if this is done, K_M^* will no longer characterize the exchange of momentum across horizontal surfaces, except at $Z = 0$.

¹ For an up-to-date review of the structure of turbulence in the planetary boundary layer, the reader is referred to Rohl (1965), Zilitinkevich *et al.* (1967) and Krauss (1968).

Across the sublayer in the real atmosphere, the stress is approximately constant and equal to its value at the surface. Accordingly, there is no wind spiralling with height across the layer and the velocity profile is logarithmic; that is

$$U(Z) = \frac{u_*}{\kappa} \log \left(\frac{Z}{Z_0} \right) \cdot \hat{U}, \quad (13)$$

where \hat{U} is a unit vector in the direction of the surface wind, $U = (U(Z), V(Z))$ is the horizontal wind vector and Z_0 is a roughness length which parameterizes the roughness of the sea surface. This leads us to consider:

Case B. In this, K_M is again taken to be constant but the no-slip condition is relaxed to one which requires that the surface stress be in the direction of the surface wind, i.e. we take

$$C_D |U(0)| U(0) = K_M^* \frac{\partial U}{\partial Z} \quad \text{at } Z=0, \quad (14)$$

where C_D is a drag coefficient, usually defined as $u_*^2/|U_{10}|^2$, where $|U_{10}|$ is the wind speed at 10 m above the mean sea level. Typical values of C_D in strong wind conditions are of the order 2×10^{-3} . Strictly, by taking this boundary condition we are neglecting the logarithmic layer and assuming the origin of Z to be somewhere near the top of the sublayer. This is not a bad approximation to make when one is interested in the total volume flux as the sublayer is much thinner than the entire inflow layer, the ratio of depths being of the order 10^{-1} to 10^{-2} .¹ The velocity profiles in this case are given by $g + if = 1 - A e^{-(1-i)\eta + i\alpha}$, where A and α are determined by condition (14) and are in

general functions of r .² This formulation can be improved by 'patching' an outer layer with constant K_M^* to a logarithmic sublayer. This is the essence of the third representation, *C*.

Case C. In this we take

$$K_M = K_M^* (1 - e^{-\kappa u_* Z / K_M^*}),$$

so that

$$K_M \sim \kappa u_* Z \quad \text{if } \kappa u_* Z / K_M^* < 1$$

and

$$K_M \sim K_M^* \quad \text{if } \kappa u_* Z / K_M^* > 1.$$

The natural surface condition for this structure of K_M is to assume that $U(Z)$ satisfies Eq. (13) in the limit as $\kappa u_* Z / K_M^* \rightarrow 0$. The solution to Eqs. (9) and (10) for this representation was obtained by Schwets (1941) and independently in a different form by Smith (1969). The velocity profiles appropriate to this case are given by $g + if = 1 - B e^{-(1-i)\eta + i\beta} F(\eta)$, where B and β are constants and $F(\eta)$ is a function which behaves like $1 + 0(\exp - \sigma \sqrt{2} \eta)$, where $\sigma > 1$, for large $\sigma \eta$. function describes the modification of the Ekman spiralling effect across the sublayer which has a relative thickness of order σ^{-1} . The profile details for this case are given in appendix B.

The most important feature of this representation is that the value of K_M^* is determined by the values of V_g , u_* and Z_0 (see eq. (iii), appendix B). In practice, there is also a functional relationship between the two non-dimensional parameters u_*/V_g and u_*/fZ_0 , that is, the surface stress is a function of the geostrophic wind and the surface roughness characteristics at a particular latitude. This relationship, which must be obtained by observation, imposes an additional constraint on the profile.

Discussion

Solutions to Eqs. (5), (6) and (7) for the hurricane boundary layer are obtained for the three representations A, B and C, assuming, in the first instance, that K_M^* does not vary with radius. In these calculations, K_M^* is taken as 7.8 m²/sec, a value obtained from Eq. (iii) of appendix B by taking $u_* = 0.14$ m/sec and $Z_0 = 1$ cm. The value for C_D in case B was taken to be 2×10^{-3} . These values are typical of the planetary boundary layer at low wind speeds.

A suitable measure of mean inflow velocity is U_{\max} , defined by the relation

$$U_{\max} = E(R/R_g) V_{gr}(R) f_{\max},$$

¹ This is contrary to the argument given in I for rejecting Rosenthal's boundary condition: it was suggested that this condition failed because the main levels of inflow are where vertical gradients of azimuthal velocity are most. This is true only if K_M is constant. In fact, the main spiralling of wind with height, which gives rise to inflow, occurs mainly in levels where vertical gradients of horizontal stress are greatest. This gradient is almost zero in the sublayer.

² Rosenthal (1962) linearized condition (14) by taking $|U(0)| = V_{gr}$. This simplifies the calculation of A and α but the physical basis for this approximation is not clear. Miller (1965) takes $|U(0)| = V(0)$ for a similar reason. We compared both these formulations with the full condition and found that the inflow layer solutions differed by not more than five per cent between the three conditions.

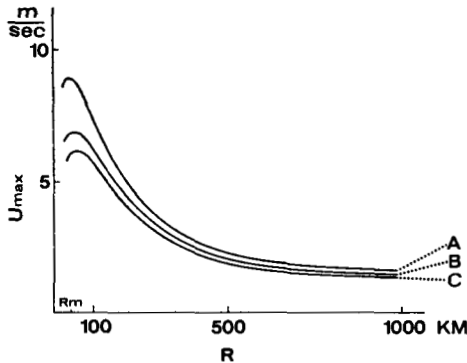


Fig. 2. Profiles of scale inflow velocity U_{\max} in the boundary layer for the cases A, B and C with K_M^* constant.

where f_{\max} is the maximum value of the profile function $f(\eta)$ (see Eq. (4)). The radial profiles of U_{\max} and of mean upflow through the top of the boundary layer W_{gr} , are shown for each of the representations A, B and C, in Figs. 2 and 3. The vertical velocity profiles, $f(\eta)$ and $g(\eta)$, are shown in Fig. 4.

As anticipated in the last section, the strongest meridional circulation induced by the friction layer occurs in the case A. The maximum upflow velocity in this case is about 37 cm/sec compared with 25 cm/sec in case B and 19 cm/sec in case C. The corresponding maximum inflow velocities are roughly 9 m/sec, 7 m/sec and 6 m/sec, respectively. Miller (1958) used observational data from several hurricanes to compute the three-dimensional wind field in these systems. In the lowest kilometer, he found mean inflow velocities of a few metres per second, reaching a maximum of about 9 m/sec

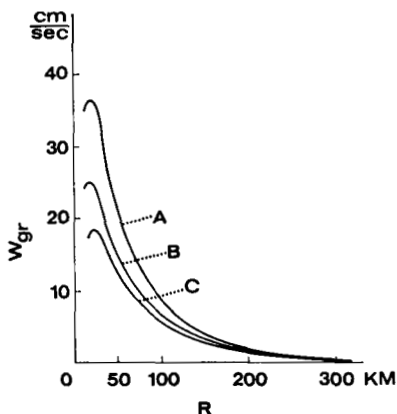


Fig. 3. Profiles of vertical velocity W_{gr} through the top of the boundary layer. Legend as for Fig. 2.

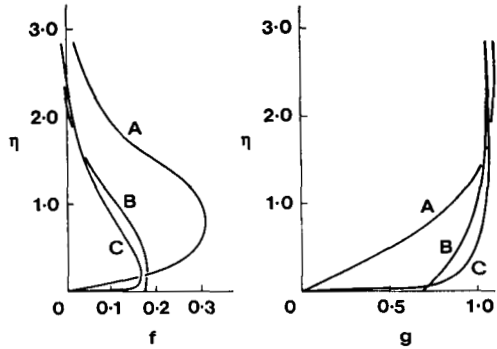


Fig. 4. Vertical profiles of radial and azimuthal velocity, f and g , in the three cases A, B and C. The profiles for B are appropriate to the geostrophic radius.

near the radius of maximum azimuthal winds. However, his estimates of mean vertical velocities show considerable variability in both horizontal and vertical directions and make comparison with the present calculations difficult. Estimates of mean upflow are also reported by Gray (1966), who analysed data obtained during a series of aircraft flights into hurricanes. Gray found values of 'a fraction of a knot' at mid-tropospheric levels, but he points out that fluctuations about these mean values are sometimes greater by an order of magnitude or two, due to individual cumulonimbus clouds. We note that our calculations give realistic values for W_{gr} , with orders of magnitude of a few tens of centimetres per second.

It does not seem possible to distinguish between the calculations in cases A, B and C on the basis of direct comparison with observation. In all cases, the predicted inflows are of the correct order of magnitude, although the exact value in case C is probably too small. However, from a meteorological standpoint one must favour this representation, as the vertical structure of turbulence and surface boundary condition approximate most closely to those which obtain in the atmosphere. Moreover, the central pressure of 940 mb, which we have taken to characterize the vortex, is fairly low and corresponds to a relatively intense storm. As a consequence, one might have expected to overestimate the maximum inflow and upflow. There is, however, one important factor which we have so far overlooked; namely, the possibility that K_M^* may vary considerably with radius. The reasons for such a belief are partly intuitive

and partly based on observation. Measurements indicate that up to moderate wind speeds, u_* is an increasing function of wind speed in the first few tens of metres above the sea surface and hence, in this region, K_M also increases at the same rate. One may therefore expect a similar increase in K_M above the sublayer, although there does not appear to be any data to indicate how rapid this increase is, especially in the annular region of high wind speeds which surrounds the core. Since the only scale velocity at our disposal in the model is $V_{gr}(R)$, we assume that K_M^* increases with decreasing R by the factor $V_{gr}(R)/V_g$. Of course, this variation is completely arbitrary but it does allow one to judge the likely importance of this effect.

Figs. 5 and 6 show the calculated inflow and upflow velocity profiles as functions of radius with this radial structure of K_M^* and in the three cases A, B and C. The overall effect of a radially decreasing eddy coefficient is to increase the strength of the meridional recirculation induced by the boundary layer and with the above variation, the strength is increased substantially. Indeed, the calculations suggest that it is more crucial to correctly parameterize radial variations in eddy coefficient rather than its vertical structure. Moreover, with the above variation of K_M^* , the third representation, C, gives the most satisfactory distributions for the inflow and upflow velocities when compared with the observations mentioned above.¹ In this case, the

¹ In this calculation, we have taken the vertical velocity profiles, f and g , as fixed. The additional complications of allowing these profiles to vary are discussed below.

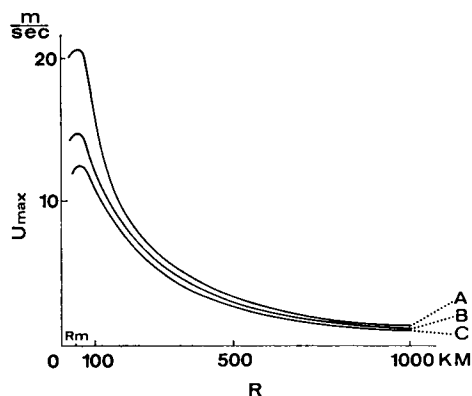


Fig. 5. Profiles of scale inflow velocity U_{max} , in the boundary layer for the cases A, B and C and with K_M^* varying radially with V_{gr}/V_g .

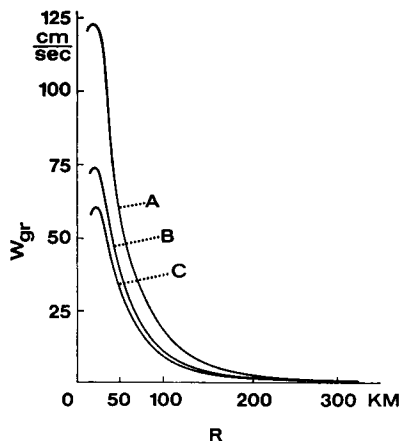


Fig. 6. Profiles of vertical velocity V_{gr} , through the top of the boundary layer. Legend as for Fig. 4.

inflow reaches a maximum of about 12 m/sec and the upflow about 60 cm/sec. Cases A and B give correspondingly larger values for these quantities.

Fig. 7 compares the profile of *scale* boundary layer thickness $\delta(R/R_g)$, in cases A, B and C, with and without radially variable K_M^* . The profiles are relatively insensitive to the vertical structure of the turbulence but there is a marked difference between the cases with different radial structure.

No attempt has been made at present to include radial variations of C_D and Z_0 in the model. Such refinements do not increase the computational difficulty, but in case C, where it is necessary to evaluate the integrals I_1 , I_2 and I_4

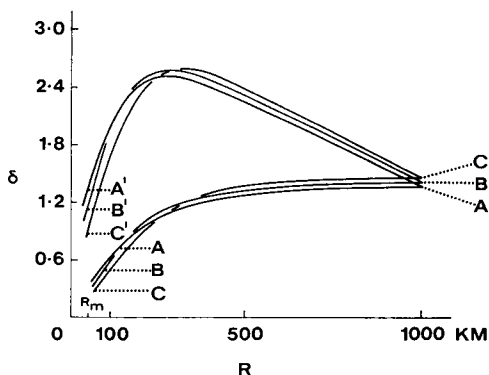


Fig. 7. Profiles of non-dimensional, scale, boundary layer thickness δ , for the cases A, B and C and for K_M^* constant and K_M^* varying radially with V_{gr}/V_g (labelled A', ... etc.).

numerically at each step of the inwards integration, the computation time is substantially increased. Although this is still within reasonable limits, it was felt that the appropriate variations for C_D and Z_0 are not sufficiently well established to warrant the extra calculations at this stage. Measurements at wind speeds less than about 12 m/sec indicate an increase in C_D and Z_0 with $|U_{10}|$ and hence with V_{gr} . However, there is a good deal of scatter in the observations (Krauss, op. cit.) and extrapolation to hurricane wind speeds is dangerous.

Conclusion

The momentum integral method appears relatively insensitive to the particular choice for the velocity profiles and is therefore suitable as a method for determining the con-

straint which is imposed by the inflow layer on the dynamics of the hurricane vortex above it. The magnitude and distribution of the induced meridional circulation depends less critically on the actual vertical structure of the turbulence than on the radial structure. Moreover, if K_M is assumed to vary with V_{gr} , estimates for the mean upflow velocity through the top of the layer compare favourably with those of observation.

Acknowledgement

The authors are grateful to Dr C. H. B. Priestley and colleagues in the Department of Meteorological Physics of C.S.I.R.O. at Aspendale, Victoria, for their interest in this work and for several stimulating discussions about it.

REFERENCES

- Davis, P. J. 1965. *Handbook of Mathematical Functions* (ed. Abramowitz & Stegun), Ch. 6. Dover, New York.
- Gray, W. M. 1966. On the scales of motion and internal stress characteristics of a hurricane, *J. Atmos. Sci.* 23, 278–88.
- Krauss, E. B. 1968. What do we not know about the sea-surface wind stress. *Bull. Amer. Met. Soc.* 49, 247–53.
- Miller, B. I. 1958. The three dimensional wind structure around a tropical cyclone. *Nat. Hurr. Res. Proj. Rep.*, no. 15, pp. 41.
- Miller, B. I. 1965. A simple model of the hurricane inflow layer. *Nat. Hurr. Res. Proj. Rep.*, no. 75, 16 pp.
- Rohl, H. U. 1965. *Physics of the Marine Atmosphere*, Ch. 4. Academic Press, New York.
- Rosenthal, S. L. 1962. A theoretical analysis of the field of motion in the hurricane boundary layer. *Nat. Hurr. Res. Proj. Rep.*, no. 56, 12 pp.
- Schwets, M. E. 1941. Determination of the coefficient of turbulent viscosity for atmospheric motions. *Proc. (Dokl.) Acad. Sci. U.S.S.R.*, 30 pp. (in German).
- Smith, R. K. 1968. The surface boundary layer of a hurricane. *Tellus* 20, 473–484.
- Smith, R. K. 1969. A parametrization of the atmospheric boundary layer. *Monash Univ. G.F.D. Lab. Paper*, no. 12.
- Zilitinkevich, S. S., Laikhtman, D. L. & Monin, A. S. 1967. Dynamics of the atmospheric boundary layer. *Izv., Atm. and Ocean. Phys.*, 3, 297–333.

APPENDIX A

In terms of the velocity profiles f and g , boundary condition (15) can be written in the form

$$V_{gr}\{f(0)^2 + g(0)^2\}^{\frac{1}{2}}(f'(0), g'(0)) = \frac{\lambda}{(2k)^{\frac{1}{2}}}(f'(0), g'(0)), \quad (i)$$

where $\lambda = K_M^*/(C_D V_g Z_g)$ is a constant and f and g are the profiles appropriate to case B. In complex form, $g + if = 1 - e^{-(1-i)\eta + i\alpha}$, where A and α are determined by (i). Thus

$$V_{gr}\{(1 - A \cos \alpha)^2 + (A \sin \alpha)^2\}$$

$$\times (1 - A e^{i\alpha}) = \frac{\lambda A}{2} \exp i \left(\alpha - \frac{\pi}{4} \right),$$

and if $A e^{i\alpha} = a - ib$, then a and b satisfy the simultaneous equations

$$\left. \begin{aligned} db &= -\lambda'(a+b) \\ d(a-1) &= -\lambda'(a+b) \end{aligned} \right\},$$

where

$$d = \{(1-a)^2 + b^2\}^{\frac{1}{2}} \quad \text{and} \quad \lambda'^2 = \lambda^2/(2k V_{gr}^2).$$

These equations may be written as

$$\left. \begin{aligned} a &= (\lambda' b + d) / (d + \lambda') \\ b &= -\lambda' a / (d + \lambda') \end{aligned} \right\}, \quad (\text{ii})$$

which may be solved by using a simple functional iteration. Initial guesses to the values of a and b are made, namely 0.5 and -0.5 respec-

tively, and a second approximation is obtained by substituting these values into the right-hand sides of Eq. (ii). This process of iteration is continued until a desired degree of convergence is reached. For Eq. (ii), the method yields six-figure convergence after thirty iterations.

APPENDIX B

Let $Z_L = K_M^* / (\kappa u_*)$ be a scale thickness for the logarithmic sublayer and write $\sigma = Z_g / Z_L$. Then, in case C, Eqs. (9) and (10) can be written in complex form

$$\frac{d}{dz} \left[(1 - e^{-\sigma z}) \frac{dq}{dz} \right] + i(q - 1) = 0, \quad (\text{i})$$

where $q = v + iu$. A particular integral of this equation is $q = 1$. With the substitution $t = e^{-\sigma z}$, the homogeneous equation becomes

$$\sigma^2 t^2 (1 - t) \frac{d^2 q}{dt^2} + \sigma^2 t (1 - 2t) \frac{dq}{dt} = iq + 0,$$

which has a power series solution,

$$q(t) = \sum_{n=0}^{\infty} a_n t^{\mu+n} \quad \text{if} \quad \sigma^2 \mu^2 = i.$$

The solution which satisfies condition (11) corresponds to the root $\mu = \sigma^{-1} e^{-i\pi/4}$ and the recurrence relation for this root gives $a_{n+1} = \{(\mu + n)(\mu + 1 + n) / (2\mu + 1 + n)(n + 1)\} a_n$. Hence the complete solution can be written

$$q(t) = 1 - T t^{\mu} {}_2F_1(\mu, \mu + 1; 2\mu + 1; t) \quad (\text{ii})$$

where T is a complex constant determined by the surface condition. For $\sigma z \ll 1$, i.e. $t = 1 - \varepsilon$ and $0 < \varepsilon \ll 1$, ${}_2F_1(\mu, \mu + 1; 2\mu + 1; t) \sim \Gamma(2\mu + 1) [H - \log t] / \{\Gamma(\mu) \Gamma(\mu + 1)\}$, where $H = 2\psi(1) -$

$\psi(\mu) - \psi(\mu + 1)$, Γ denotes the gamma function with complex argument and ψ is its logarithmic derivative. Thus if $z_0 = Z_0 / Z_g$, the solution (ii) satisfies condition (14) in non-dimensional form if $T = \Gamma(\mu) \Gamma(\mu + 1) / \{\Gamma(2\mu + 1) (\log(\sigma z_0) - H)\}$ and if σ satisfies the equation

$$\kappa V_g - u_* [H - \log(\sigma z_0)] = 0 \quad (\text{iii})$$

Hence, given u_* , z_0 and V_g , which may in practice be relatively easily obtained, the value of K_M^* can be obtained from Eq. (iii) by iteration. The profiles f and g , defined by Eq. (13), are given in complex form by

$$g + if = 1 - B e^{-(1-t)\eta + i\beta} F(\eta), \quad (\text{iv})$$

where

$$B e^{i\beta} = T$$

and $F(\eta) = {}_2F_1(\mu, \mu + 1; 2\mu + 1; \exp -\sigma \sqrt{2}\eta)$.

For large $\sigma\eta$, $F(\eta) \sim 1 + 0(\exp -\sigma \sqrt{2}\eta)$ and the profiles, together with the integrals $I_1 \rightarrow I_s$ in (8) are most easily obtained by taking a large value of η , say $\eta_0 = 5/\sigma$ and integrating the differential equations for f and g inwards from η_0 to zero. The starting values are obtained from Eq. (iii), assuming $F(\eta_0) = 1$. The values of $\Gamma(\mu)$, $\psi(\mu)$ etc., are easily calculated from the asymptotic expansions and recurrence formulæ for these functions—see for example Davis (1965).

ПРИВОДНЫЙ ПОГРАНИЧНЫЙ СЛОЙ ТАЙФУНА

Часть II

В предыдущей статье одним из авторов (Смит, 1968) был предложен метод моментов для исследования главных особенностей приводного слоя трения в стационарном, осесимметричном тайфуне, который определяется радиальным изменением давления вблизи поверхности моря. Так, путем выбора соответствующих вертикальных профилей радиальной и тангенциальной скорости в пограничном слое этот метод дает оценку для радиального распределения среднего притока массы, толщины пограничного слоя и среднего уходящего потока через верхнюю границу слоя. Теория, таким образом, дает связь между слоем притока и самим вихрем. В настоящей работе предложенный метод используется для исследования влияния турбулентной структуры на характеристики пограничного слоя. Турбулентность характеризуется коэффициентом вязкости K_M ; сравниваются решения, соответствующие моделям с разными профилями K_M и граничными

условиями. Модели изменяются от самых простых, когда коэффициент K_M постоянен, а на поверхности ставится условие прилипания, до более сложных, когда K_M изменяется по вертикали и по радиусу и меняется с высотой линейно на протяжении нескольких десятков метров над уровнем моря. Решения показывают, что в тайфунах в действительности возрастание K_M в сторону области максимального ветра приводит к значительному возрастанию притока массы по сравнению с аналогичным слоем, в котором K_M не меняется по радиусу. Кроме того, радиальный профиль толщины пограничного слоя сильно отличается в двух случаях. Сравниваются решения для трех граничных условий у поверхности; найдено, что скорости притока и оттока массы через верхнюю границу при данном радиусе возрастают с возрастанием приземного трения. Исправлена ошибка вычислений в первой части.